21st International Conference on Pattern Recognition (ICPR 2012)
November 11-15, 2012. Tsukuba, Japan

Human Identification from *at-a-distance* Images by Simultaneously Exploiting Iris and Periocular Features

Chun-Wei Tan, Ajay Kumar
Department of Computing, The Hong Kong Polytechnic University, Kowloon, Hong Kong
Email: *cwtan@ieee.org, ajaykr@ieee.org*

Abstract

Iris recognition from at-a-distance *face images has high applications in wide range of applications such as remote surveillance and for civilian identification. This paper presents a completely automated joint iris and periocular recognition approach from the face images acquired at-a-distance. Each of the acquired face images are used to detect and segment periocular images which are then employed for the iris segmentation. We employ complex texture descriptors using Leung-Mallik filters which can acquire multiple periocular features for more accurate recognition. Experimental results presented in this paper achieve 8.1% improvement in recognition accuracy over the best performing approach among SIFT, LBP and HoG presented in the literature. The combination of simultaneously segmented iris and periocular images achieves average rank-one recognition accuracy of 84.5%, i.e., an improvement of 52% than those from only using iris features, on independent test images from 131 subjects. In order to ensure the repeatability of the experiments, the CASIA.v4-distance, i.e., a publicly available database was employed and all the 142 subjects/images were considered in this work.*

1. Introduction

Iris recognition has been emerging as one of the most preferred biometric modalities for the automated personal identification. The complex iris patterns provide highly discriminative features which can ensure reliable human identification. It is widely believed that complex iris patterns are relatively stable[*] during person's lifetime [1]-[3]. A typical iris recognition system comprises of the following modules: (1) image acquisition (2) iris segmentation and (3) normalization (4) feature extraction and (5) matching. Each of these modules has been extensively studied over the years and has matured to generate robust performance from the eye images acquired under near infrared illumination.

The image acquisition module primarily consists of imaging hardware/sensor which typically synchronize the image acquisition with the near-infrared (NIR) illumination, typically in the wavelength range of 700-900 nm, to ensure sufficient quality of iris images that can reveal the iris texture. The images are usually acquired within proximate distance from 1-3 feet in a controlled environment [2], [4]. Increasing demand for the development of high security applications, such as remote surveillance, has motivated several research efforts to extend the standoff distance[†]. Reference [5]-[6] are some examples of such ongoing projects for the long-range image acquisition which support the standoff distances up to 8 meters. In this paper, we performed rigorous experiments to evaluate the automated iris recognition performance using a combination of simultaneously acquired/segmented iris and periocular features.. The iris and periocular images are automatically segmented from the face images acquired *at-a-distance* of ~ 3 meters from the camera. The database employed is publically available from [7]. We attempt to exploit Leung-Malik filters (LMF) which can acquire wide-range of local features from the segmented periocular images. The LMF are the set of the filters which have shown to be effective in simultaneously extracting distinctive features from the complex textured patterns and can also be effective to characterize complex periocular region. The experimental results illustrated in this paper suggest that the combination of simultaneously segmented iris and periocular features can achieve average rank-one accuracy of *83%* on publicly available *CASIA v4-distance* database. Achieved results also suggest average improvement of iris recognition performance by *52%* as compared to the case when only iris features (without periocular details) are employed.

The remainder of this paper is organized as follows. In section 2, we present the details of the automated approach for the simultaneous iris and periocular image segmentation from the distantly acquired face

[*] Recent study in [19] suggests template aging effect for the iris biometrics.

[†] The distance between acquisition subject and the camera.

images. The section 3 presents the evaluation protocol and the experimental results from the experiments. Finally, the discussion and key conclusions from this study is summarized in section 4 of this paper.

2. Joint Iris and Periocular Recognition

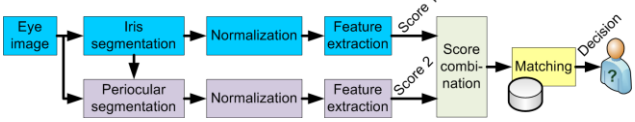

Figure 1: Improved iris recognition using simultaneous combination of periocular features

The block diagram for simultaneously exploiting iris and periocular features from the distantly acquired face images, as investigated in this paper, is shown in Figure 1.

2.1. Iris segmentation

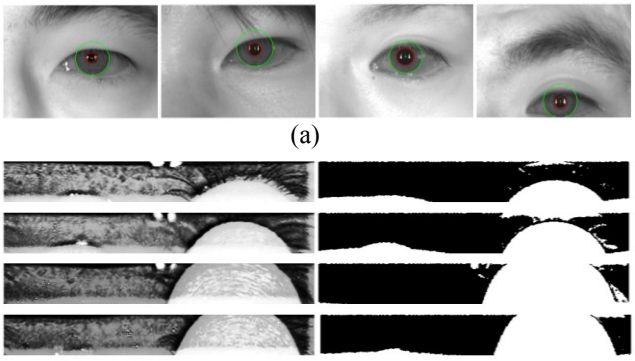

(a)

(b)

Figure 2: Iris segmentation. (a) samples of the segmented iris images, (b) samples of the normalized iris images and their corresponding masks.

An improved version of the iris segmentation method as proposed in [3] is adopted due to its superior performance to be employed for online system. Firstly, the input iris image is binarized using a weighted Otsu's method [17] before performing line scanning to localize the pupil. Such binarization step saves the requirement for determining the hard threshold as in [3]. For each of the candidate line in the binarized image B, the candidate pupil centers $(\boldsymbol{x_p}, \boldsymbol{y_p})$ are assumed to be within a small window which centered at the middle of each line. In order to search for an optimal center, a voting scheme is adopted by counting the radial edge points from the edge map generated using the Canny edge detector. The candidate center with radius R_p which produces the largest voting score is then employed as the optimal pupil center. The iris boundary can be localized in a similar manner by searching the optimal iris center (x_i, y_i) and radius R_i around a small window centered at (x_p, y_p). Figure 2 illustrates some samples of the detected eye images, along with their correspondingly segmented normalized iris images and their respective iris image masks.

2.2. Periocular region segmentation

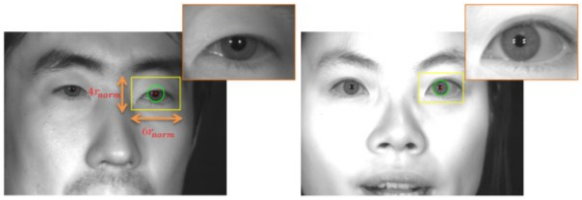

Figure 3: Image samples from the automatically segmented periocular region (left eyes) images

Periocular is referred to the region around the eye [13]. Currently, there is no clear definition about the size of the periocular region. Therefore, we adopted the approach as similar to [13] for segmenting the periocular region with respect to the segmented iris information (x_{ir}, y_{ir}, r_{ir}). Firstly, the input image is normalized (upscaling/downscaling) based on a scale factor, $s_f = {}^{r_{norm}}/_{r_{ir}}$, where r_{norm} is the normalized iris radius. Note that the (x_{ir}, y_{ir}) is shifted due to the normalization process and the resultant center can be computed as $(\widetilde{x_{ir}}, \widetilde{y_{ir}}) = s_f(x_{ir}, y_{ir})$. The periocular region Ω_{pe} defined as the rectangular region of size $W \times H$ centered at $(\widetilde{x_{ir}}, \widetilde{y_{ir}})$. The W and H denote the width and the height of Ω_{pe}, which are calculated as $W = 6r_{norm}$ and $H = 4r_{norm}$. Figure 3 illustrates some sample images from the segmented results of the periocular region from the face images.

3. Experimental Results

- **Database**

CASIA.v4-distance [7]: The full database consists of a total of 2567 images from 142 subjects. Face images from subjects were acquired at-a-distance of ~3 meters from the camera and the acquisition was performed using NIR imaging. Images from the first 10 subjects were employed as training images while the images from subjects 11 – 141 were employed as test images. In this work, the *first eleven left eye* images only were considered. The left eye images were automatically extracted using the AdaBoost eye detector [8], [9].

- **Features extraction and matching**

Iris: The segmented iris images were normalized into 512 × 64 pixels based on the rubber-sheet model [2]. The normalized images were enhanced using the non-linear enhancement technique as in [3]. Log-Gabor filter [10] was employed to extract discriminant iris features from the enhanced normalized images.

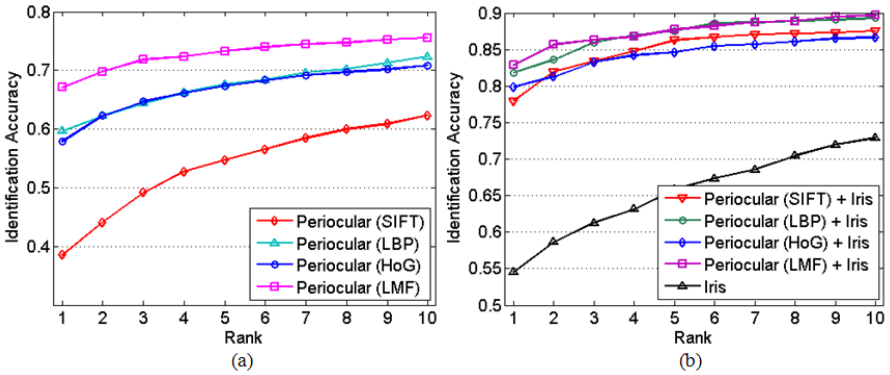

Figure 6: CMC from (a) periocular features, (b) match score combination of periocular and iris features

The two major parameters *wavelength* and *SigmaOnf* were respectively set to 20 and 0.25. Hamming distance was used as the distance metric to compute the matching scores.

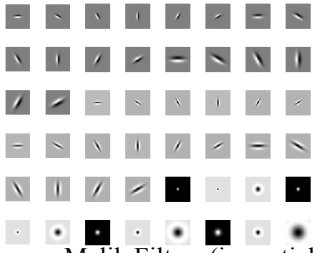

Figure 4: Leung-Malik Filters (in spatial domain)

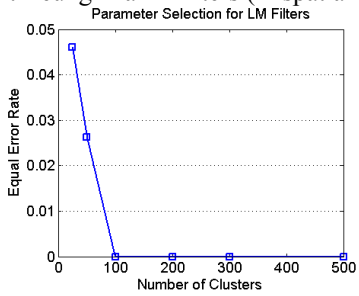

Figure 5: Training of *k*-texton dictionary

Periocular: Periocular features were extracted using Leung-Malik filters (LMF) which is inspired from their success in achieving superior performance for texture classification in [11]. LMF is a set of filters constructed from Gaussian derivative at different orientations and scales, Laplacian of Gaussian and Gaussian filters as illustrated in Fig. 4. Such filters are employed to extract distinct and multiple texture features from segmented periocular regions. Firstly, the filter responses from the training images are clustered using *k*-means clustering [15] in order to construct the texton dictionary. The cluster (textons) which produces the lowest EER (equal error rate) is then employed to classify filter responses from the test images. As can be observed in Figure 5, the parameter *k* stabilizes from *100*-cluster onwards. Therefore the texton dictionary which consisted of 100 textons was constructed. Chi-square distance was employed as the metric to compute the matching scores.

- **Score combination**

In order to consolidate matching scores from two different matching distances, score normalization is necessary as a priori. The min-max normalization scheme was used for the matching scores computed from the iris and periocular images. The normalized iris and periocular scores, $\grave{s}_{iris}$ and $\grave{s}_{periocular}$, are then combined using weighted sum method, *i.e.* $S = \omega_1 \grave{s}_{iris} + \omega_2 \grave{s}_{periocular} : \omega_1 + \omega_2 = 1$.

- **Performance evaluation**

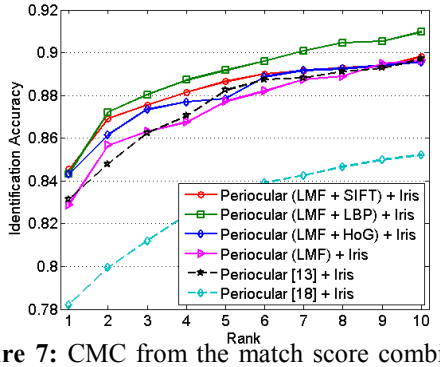

Figure 7: CMC from the match score combination of multiple periocular features and the iris image features

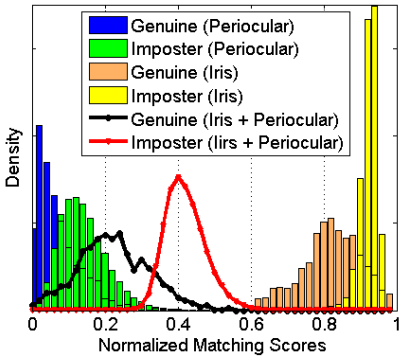

Figure 8: Distribution of the matching scores from iris and periocular features

The recognition performance of the investigated approach can be observed from the CMC (Cumulative Match Characteristic) curves in Figure 6. Figure 6(a) presents the exclusive evaluation of the periocular biometrics and the comparison with the state-of-the-art methods [12]-[16]. It can be observed that the developed method significantly outperforms the other methods of periocular recognition by an average of 34%. An average improvement of 3.8% from the developed approach is also observed for the joint periocular and iris scores. The fusion of the proposed periocular and iris features has shown significant improvements of 52% (rank-one) as compared to the case when only iris features are utilized. We also performed performance evaluation from the score combination of iris and periocular features and the results are shown in Figure 7. It may be noted that we have not masked the iris region pixels in the periocular images. In this context, the study in [13] suggests that the performance from periocular images using iris masking and without iris masking is quite similar. The simultaneously generated distribution of the genuine and imposter scores from the iris and the best performing periocular features (LMF + LBP) is shown in Figure 8. The best rank-1 recognition rate of 84.5% is observed from the combination of LMF, SIFT and iris features. Our feature extraction and matching strategy achieves an average improvement of 4.8% in rank-one recognition accuracy as compared to the existing competing approaches in [13], [18].

4. Conclusions and Future Work

This paper has investigated a completely automated approach for human identification using distantly acquired iris images which simultaneously exploits iris and periocular features. The experimental results presented in this paper illustrate average rank-one recognition rate of 83% from the score combination of periocular (LMF) and iris features, which suggests an improvement of 52% over the case when only iris features are employed. The score combination from multiple features exploited in this paper achieves marginal improvement, *i.e*. the rank-one recognition accuracy jumps to 84.5%. The further work in this area should focus on improving the iris segmentation performance and also consider the information from both eyes to further improve the accuracy.

Acknowledgement: Authors thankfully acknowledge the use of CASIA V4-at-distance database from [7].

References

[1] K. Miyazawa K, K. Ito, T. Aoki, K. Kobayashi and H. Nakajima, "An Effective Approach for Iris Recognition Using Phase-Based Image Matching," *IEEE Trans. Pattern Anal. Mach. Intell.*, vol.30, pp.1741-1756, 2008.

[2] J. Daugman, "How iris recognition works," *IEEE Trans. Circuits Syst. Video Technol.*, vol. 14, pp. 21–30, 2004.

[3] A. Kumar and A. Passi, "Comparison and combination of iris matchers for reliable personal identification," *Pattern Recognit.*, vol.43, no.3, pp.1016-1026, 2010.

[4] K. Bowyer, K. Hollingsworth, and P. Flynn, "Image understanding for iris biometrics: A survey," *Image & Vision Computing*, vol. 110, no. 2, pp. 281–307, 2008.

[5] J.R. Matey, O. Naroditsky, K. Hanna, R. Kolczynski, D.J. LoIacono, S. Mangru, M. Tinker, T.M. Zappia, W.Y. Zhao, "Iris on the Move: Acquisition of Images for Iris Recognition in Less Constrained Environments," *Proc. of the IEEE*, vol.94, no.11, pp.1936-1947, 2006.

[6] S. Venugopalan, U. Prasad, K. Harun, K. Neblett, D. Toomey, J. Heyman, and M. Savvides, "Long Range Iris Acquisition System for Stationary and Mobile Subjects," *Proc. IJCB 2011*, pp.1–8, 2011.

[7] Biometrics Ideal Test. http://biometrics.idealtest.org/dbDetailForUser.do?id=4

[8] G. Bradski, "The OpenCV Library," Dr. Dobb's Journal of Software Tools, 2000.

[9] P. Viola and M. Jones, "Rapid object detection using a boosted cascade of simple features," *Proc. CVPR 2001*, pp. 511–518, 2001.

[10] L. Masek and P. Kovesi, *MATLAB Source Code for a Biometric Identification System Based on Iris Patterns*, The University of Western Australia. 2003. http://www.csse.uwa.edu.au/~pk/studentprojects/libor/.

[11] T. Leung and J. Malik, "Representing and recognizing the visual appearance of materials using three-dimensional textons," *International Journal of Computer Vision*, vol. 43, no. 1, pp. 29–44, 2001.

[12] V. P. Pauca, M. Forkin, X. Xu, R. Plemmons and A. Ross, "Challenging Ocular Image Recognition," *Proc. SPIE (Biometric Technology for Human Identification VIII)*, vol. 8029 80291V-1 – 80291V-13, 2011.

[13] U. Park, R. R. Jillela, A. Ross, and A. K. Jain, "Periocular biometrics in the visible spectrum," *IEEE Trans. Info. Forensics & Security*, vol. 6, 2011.

[14] D. G. Lowe, "Distinctive image features from scale-invariant keypoints," *International Journal of Computer Vision*, vol. 60, no. 2, pp. 91–110, 2004.

[15] VLFeat: An Open and Portable Library of Computer Vision Algorithms. http://www.vlfeat.org/

[16] T. Ojala, M. Pietikainen, and T. Maenpaa, "Multiresolution gray-scale and rotation invariant texture classification with local binary patterns," *IEEE Trans. Pattern Anal. Mach. Intell.*, vol. 24, pp. 971–987, 2002.

[17] N. Otsu, "A Threshold Selection Method from Gray-Level Histograms," *IEEE Systems Man and Cybernetics*, vol.9, no.1, pp.62-66, 1979.

[18] D.L. Woodard, S.J. Pundlik, J.R. Lyle and P.E. Miller, "Periocular region appearance cues for biometric identification," *Proc. CVPRW 2010*, pp.162-169, 2010.

[19] S. P. Fenker and K. W. Bowyer, "Analysis of template aging in iris biometrics," *Proc. CVPR 2012*, Providence, CVPRW'12, June 2012.